ELSEVIER

Ceramics International 29 (2003) 83–89

CERAMICS INTERNATIONAL

www.elsevier.com/locate/ceramint

Microstructure and mechanical properties of machinable $Al_2O_3/LaPO_4$ composites by hot pressing

Ruigang Wang*, Wei Pan, Jian Chen, Minghao Fang, Mengning Jiang, Zhenzhu Cao

State Key Lab of New Ceramics and Fine Processing, Department of Materials Science and Engineering, Tsinghua University, Beijing 100084, People's Republic of China

Received 5 February 2002; received in revised form 30 April 2002; accepted 6 June 2002

Abstract

$Al_2O_3/LaPO_4$ composites were fabricated by hot-pressing, and the microstructure and mechanical properties were investigated. The layered $LaPO_4$ grains inhibited densification of the composites and grain growth of Al_2O_3 due to the decreasing grain boundary diffusivity and mobility. Compared with monolithic Al_2O_3, the composite system possessed narrow and homogeneous grain size distribution, and this tendency became more obvious with increasing $LaPO_4$ content. However, the fine and homogenous microstructure did not improve the fracture strength and elastic modulus due to formation of weak bonding between Al_2O_3 and $LaPO_4$. Flexural strength and Vickers hardness of the $Al_2O_3/LaPO_4$ composite added with 40 wt.% $LaPO_4$ and sintered at 1450 °C reached 331 MPa and 4.69 GPa, respectively. It was shown that the machinability of alumina matrix materials could be greatly improved after introducing an interface dispersion phase of layer-structured $LaPO_4$.

Keywords: B. Microstructure; C. Mechanical properties; D. Al_2O_3; $LaPO_4$; Machinability

1. Introduction

$LaPO_4$ (lanthanum phosphate, monazite) is a suitable and effective oxide interphase material, which exhibits high stability at high temperature in both reducing and oxidizing environments and good chemical compatibility with Al_2O_3 [1–3]. The $LaPO_4/Al_2O_3$ interface is weak enough to prevent crack growth by interfacial debonding and crack deflection. Recently, according to the research of Davis et al. [4], two-phase composites consisting of $LaPO_4$ or $CePO_4$ and alumina, mullite, or zirconia were cut and drilled using conventional tungsten carbide metal-working tools. $LaPO_4$ in the $Al_2O_3/LaPO_4$ composites was quite stable and no reaction occurred between the two phases up to 1600 °C, provided the La:P ratio in the monazite is close to 1. Recently, $LaPO_4$ ceramics were fabricated in our group by different sintering methods (pressureless sintering, hot pressing and spark plasma sintering) and layered crystal structure $LaPO_4$ grains were observed [5]. Therefore, $Al_2O_3/LaPO_4$ system can be a good candidate material for machinable ceramics due to the presence of weak bonding between lanthanum phosphate and alumina, and layer-structured $LaPO_4$ phase.

In this paper, we have carried out a systematic investigation of the microstructure and mechanical properties of $Al_2O_3/LaPO_4$ composites with different $LaPO_4$ addition. The studies revealed that monazite-type $LaPO_4$ was compatible with the Al_2O_3 phase and also had favorable mechanical and machining properties in terms of prolonging the crack route, interfacial debonding and crack deflection.

2. Experimental procedures

2.1. Powder preparation and sintering

$LaPO_4$ powders were synthesized by mixing phosphoric acid with lanthanum oxide in a water bath. Lanthanum oxide was dissolved in a diluted phosphoric acid at the La to P of 1:1 in order to achieve $LaPO_4$ as a final product. The direct reaction between lanthanum oxide

* Corresponding author. Tel.: +86+10-62772859; fax: +86-10-62771160.

E-mail address: rgwang99@mails.tsinghua.edu.cn (R. Wang).

0272-8842/02/$22.00
PII: S0272-8842(02)00093-7

and phosphoric acid was a clean reaction with no by-products other than water and followed by the reaction

$$La_2O_3 + 2H_3PO_4 \rightarrow 2LaPO_4 + 3H_2O \quad (1)$$

La_2O_3 powders were slowly added to 85% H_3PO_4 (diluted by distilled water), and large precipitates formed immediately at the reaction site. Subsequently, the synthesized powders were washed several times with de-ionized water until the pH value of the filtered water became close to 7. La_2O_3 powders of analytical grade (purity > 99.99%, 0.2 μm, General Research Institute For Non-ferrous Metals, China) were used as raw material in this experiment.

The dried $LaPO_4$ powders were calcined at different temperatures to determine a suitable temperature for obtaining powders with pure phase and fine grain size. The powders calcined at 1000 °C for 2 h were re-milled and sieved using a 100-mesh screen. The composite powders with different $LaPO_4$ addition were ball-milled under ethyl alcohol with agate balls for 24 h and then dried, sieved using a 100-mesh sieve. Pure Al_2O_3, $LaPO_4$ and mixtures of Al_2O_3 and $LaPO_4$ (10, 20, 30, 40 wt.%) were uniaxially dry-pressed at 100 MPa to disks of 50mm in diameter, and then hot-pressed in graphite dies in nitrogen atmosphere at 1450° for 2 h. The sintering profile followed the schedule: room temperature to 1200 °C, 10 °C/min, 1200 to 1450 °C, 5 °C/min, hold at the sintering temperature for 2 h, followed by natural cooling by continued water circulating cooling system of the furnace.

2.2. Characterization of microstructure and mechanical properties

XRD was carried out to investigate the chemical compatibility of Al_2O_3 and $LaPO_4$ phase at the sintering temperature using an X-ray diffractometer (Cu-Kα, Model Rigaku Automated D/Max-rb, Japan). Bulk density was measured by the Archimedes method. Hardness values were determined on polished samples by using a load 50N in a micro-hardness tester fitted with a Vickers indenter. Five indents were made for each sample. The hardness was deduced from the diagonal width ($2a$) of the indentation and the contact load (P) by the following equation

$$H = \frac{1854.4 \cdot P}{(2a)^2} \quad (2)$$

The flexural strength was measured by the three-point bending method with specimen dimensions of 36×4×3 mm ^{3}, a bending span of 30 mm, and a cross-head speed of 0.5 mm/min at room temperature. The tensile surface of the sample was polished with diamond paste down to 0.5 μm and the long edges of the tensile surface were rounded. Elastic modulus (E) was measured by load-displacement curve on specimens 36×4×3mm^3 using an A-2000 Shimadzu universal materials testing machine with a crosshead speed of 0.05 mm/min. Fracture surfaces of the composites were observed under scanning electron microscopy, using SEM LEO 1530, Germany.

3. Results and discussion

3.1. Synthesis of $LaPO_4$ powders

The product of the solid–liquid reaction was amorphous phase and possessed some impurity phase, which need further calcinations. The phase-evolution characteristics of the as-received powders were studied in air at various calcining temperatures (700–1200 °C) by powder X-ray diffraction and scanning electron microscope. Fig. 1 showed the XRD spectra of as-received $LaPO_4$ powders calcined at different temperatures. According to the XRD results, the as-received powders were amorphous phase, and this result was confirmed by observation of the particle morphology by SEM. Moreover, some of the additional peaks of as-received powders could not be matched with the peaks of the monolithic $LaPO_4$. However, the powders calcined at 1000 °C showed broad peaks of lanthanum phosphate (monazite structure) (JCPDS 320493) and pure phase with sharp peaks were obtained above 1000 °C. The peaks of the calcined powders at 1000 °C for 2 h were clearly observed indicating that the samples were crystallized. The XRD pattern of the $LaPO_4$ powders calcined at 1200 °C for 2 h was similar to that of the powders calcined at 1000 °C for 2 h, except the peaks became much sharper. According to the Scherrer formula [6], the grain size of particles was increased with increasing calcining temperature.

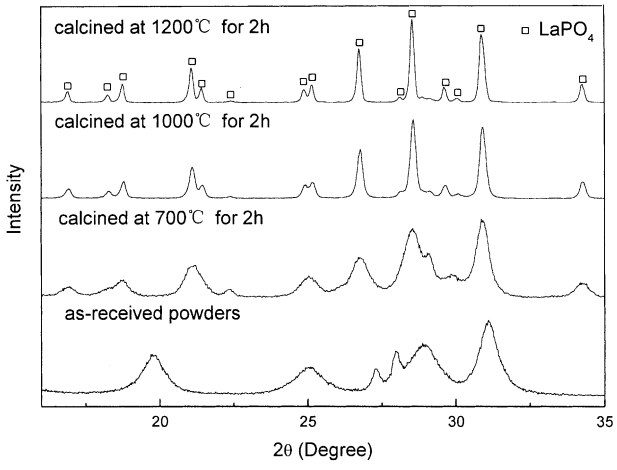

Fig. 1. XRD patterns of $LaPO_4$ powders calcined at different temperatures.

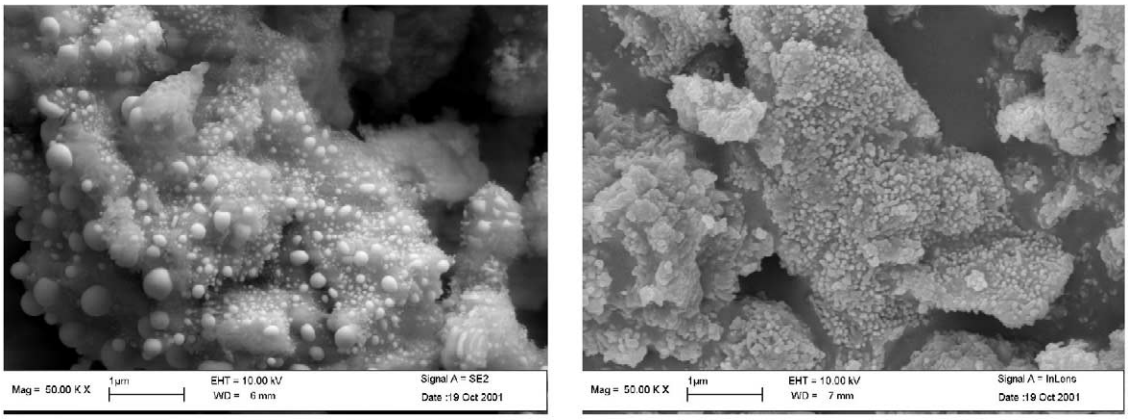

(A)As-received powders (B) Powders calcined at 1000C° for 2h

Fig. 2. Morphology of as-received powders and calcined powders at 1000 °C for 2 h.

Fig. 2 showed the SEM morphology-evolution characteristics before and after calcining, in which the as-received powders revealed amorphous phase, as proved by the result of XRD. The as-received powders were agglomerated and basically irregular in shape, with an indefinite particle size. After calcining at 1000 °C for 2 h, $LaPO_4$ powders with fine grain size and high crystallization were obtained.

3.2. Compatibility and sinterability

Fig. 3 showed the XRD patterns of $Al_2O_3/LaPO_4$ composites with different $LaPO_4$ content sintered at 1450 °C for 2 h in the parallel and perpendicular surface to hot pressing direction. In the hot-pressed materials synthesized here the only phase detected by X-ray diffraction were Al_2O_3 and $LaPO_4$. It was observed in this figure that independent of the $LaPO_4$ concentrations, no other crystalline phase up to 1450 °C by hot pressing was observed indicating that no reaction occurred at this sintering temperature. The preferred orientation was illustrated clearly by X-ray diffraction result according to the ratio of (200) and (012) peak area used as a parameter of layered $LaPO_4$ grain orientation.

According to Table 1, although due to high density of $LaPO_4$ ($\rho = 5.07$ g/cm^3), the bulk density of composites increased with increasing $LaPO_4$ addition, at the same time the relative density of composites decreased compared with pure Al_2O_3 and $LaPO_4$ ceramic. It was indicated that sinterability of composites reduced with $LaPO_4$ addition. Therefore, layered $LaPO_4$ addition reduced the sinterability of $Al_2O_3/LaPO_4$ composites, leading to a decrease of mechanical properties of composites.

Table 1
Sintered densities of $Al_2O_3/LaPO_4$ composites by hot-pressing at 1450 °C

Content of $LaPO_4$	Bulk density (g/cm^3)	Theoretical density (g/cm^3)	Relative density (% Th[a])
0	3.94	3.99	98.7
10	3.94	4.08	96.7
20	4.08	4.17	97.9
30	4.18	4.26	98.1
40	4.20	4.36	96.2
100	5.01	5.07	98.8

[a] Theoretical density: $\rho Al_2O_3 = 3.99$ g/cm^3; $\rho_{LaPO_4} = 5.07$ g/cm^3.

3.3. Mechanical properties

Fig. 4 showed influence of $LaPO_4$ content on the bending strength of $Al_2O_3/LaPO_4$ composites. Incorporating $LaPO_4$ particles remarkably reduced the fracture strength of Al_2O_3. The monolithic Al_2O_3 sintered 1450 °C exhibited a maximum strength of 550 ± 32 MPa, while the strength of 40 wt.%$Al_2O_3/LaPO_4$ composite and $LaPO_4$ ceramic are 331 ± 41 and 137 ± 18 MPa, respectively. Due to the weak bonding between Al_2O_3 and $LaPO_4$ and layered soft $LaPO_4$ phase, therefore, it was evident that microstructure greatly affected the mechanical properties such as fracture strength, elastic modulus and hardness.

Generally, the refinement of the matrix grain size and homogeneity in the matrix grain size distribution will result in improvement of mechanical properties [7]. It is well known that the strength is proportional to (maximum grain size)$^{-1/2}$. However, due to the weak bonding of Al_2O_3 and $LaPO_4$ and layered soft $LaPO_4$ phase, the fine and homogeneous microstructure by $LaPO_4$ addition and low densification resulted in the reduction of mechanical properties of the composites.

Fig. 5 showed the variation of elastic modulus of the composites with increasing $LaPO_4$ addition. The decrease of elastic modulus is attributed to the addition of $LaPO_4$ particulate with lower elastic modulus than Al_2O_3 and can be explained by using the rule of mixture.

The most important advantage of $Al_2O_3/LaPO_4$ composites is that they possess excellent machinability. Hardness is an important parameter as an indication of

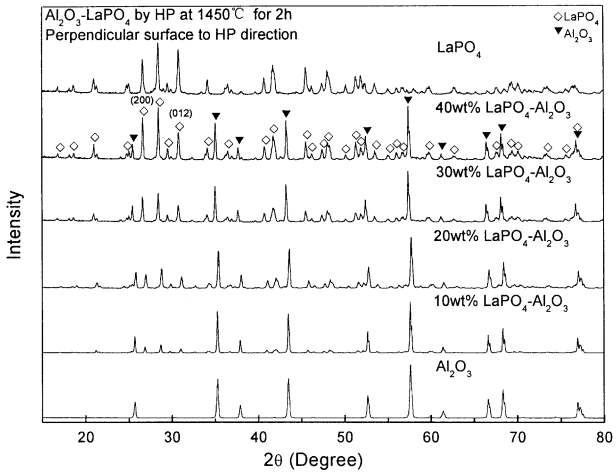

(a) Perpendicular to hot pressing direction

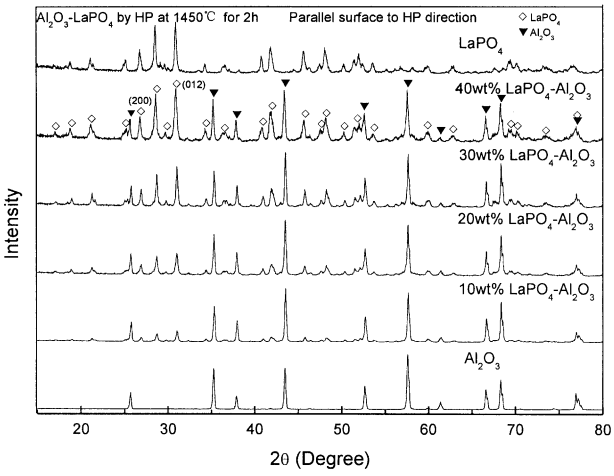

(b) Parallel to hot pressing direction

Fig. 3. XRD patterns of $Al_2O_3/LaPO_4$ composites sintered by HP at 1450 °C for 2 h for parallel and perpendicular surface to hot pressing direction.

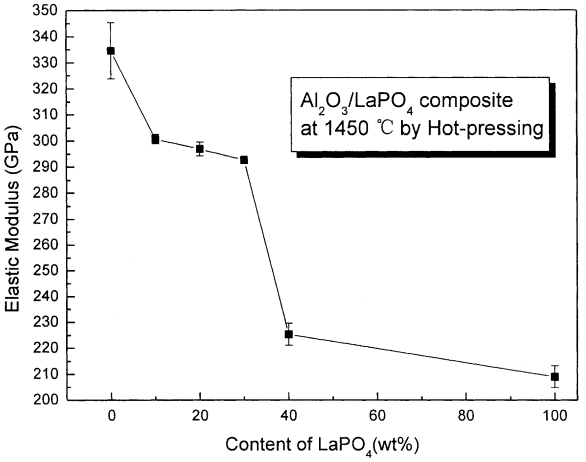

Fig. 5. Effects of $LaPO_4$ content on elastic modulus of $Al_2O_3/LaPO_4$ composites.

ceramic machinability. Generally, lower is the hardness, more excellent is the machinability. Fig. 6 showed the effects of $LaPO_4$ content on the hardness change of $Al_2O_3/LaPO_4$ composites. Generally, the decrease of hardness can be attributed to the crack deflection at crack tip, blunting and bridging at process zone wake by second phase. In this system, the crack propagated along weak bonding of Al_2O_3 and $LaPO_4$ and layer flat of $LaPO_4$ phase. Therefore the improved crack deflection ability may contribute to the machinability improvement in the composites. The Vickers hardness of 40 wt.% $Al_2O_3/LaPO_4$ composite and $LaPO_4$ was 4.69 ± 0.01 and 4.48 ± 0.18 GPa, respectively. Those values are close to that of machinable mica glass-ceramic (3 GPa) [8] and layered ternary compounds Ti_3SiC_2 (4–5 GPa) [9]. That indicated $LaPO_4$ ceramic and 40 wt.% $Al_2O_3/LaPO_4$ composite could possess excellent machinability.

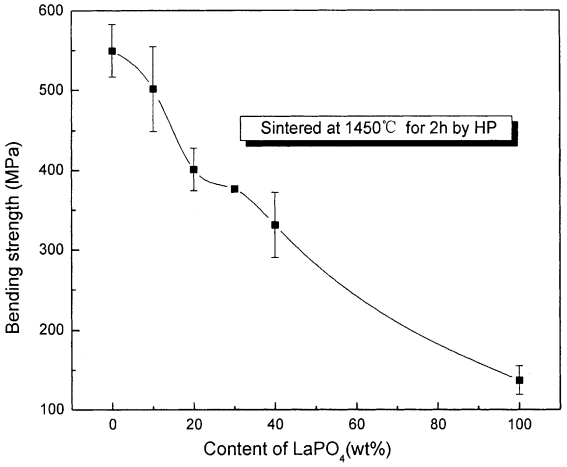

Fig. 4. Effect of $LaPO_4$ content on the bending strength of $Al_2O_3/LaPO_4$ composites.

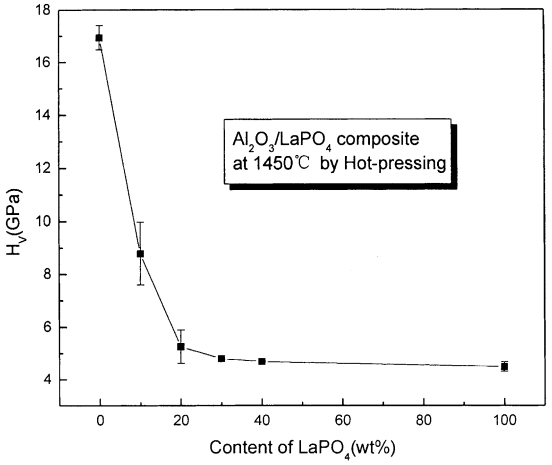

Fig. 6. Effect of $LaPO_4$ content on the Vickers's hardness $Al_2O_3/LaPO_4$ composites.

3.4. Microstructure observation

Scanning electron micrographs illustrating the microstructures of $Al_2O_3/LaPO_4$ composites with different $LaPO_4$ addition were shown in Fig. 7. As shown in Fig. 7(a), for pure Al_2O_3, the grain sizes were about 1 μm, at the same time there existed some abnormal grain growth. However, for the 40 wt.% $Al_2O_3/LaPO_4$ composite, the grain size of alumina were 0.5 μm. SEM observation of composites indicated that the addition of $LaPO_4$ impeded the grain growth of Al_2O_3. The dependence of the grain size on the second phase content can be explained by using Zener's equation, which suggests a relationship between grain size of matrix and volume fraction and particle size of the second phase

$$G = k(r/f) \tag{3}$$

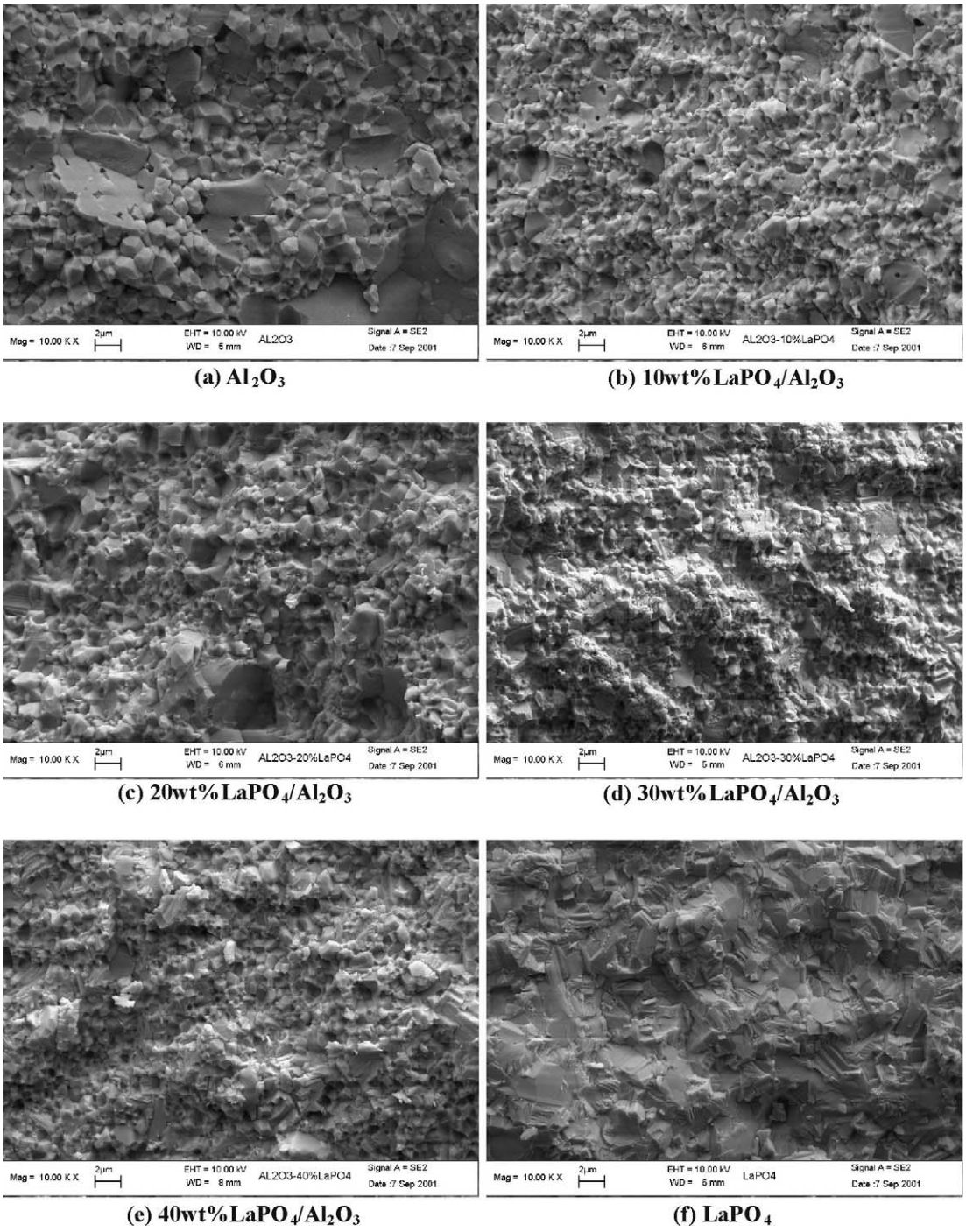

Fig. 7. SEM images of fracture surface for $Al_2O_3/LaPO_4$ composites with different $LaPO_4$ addition.

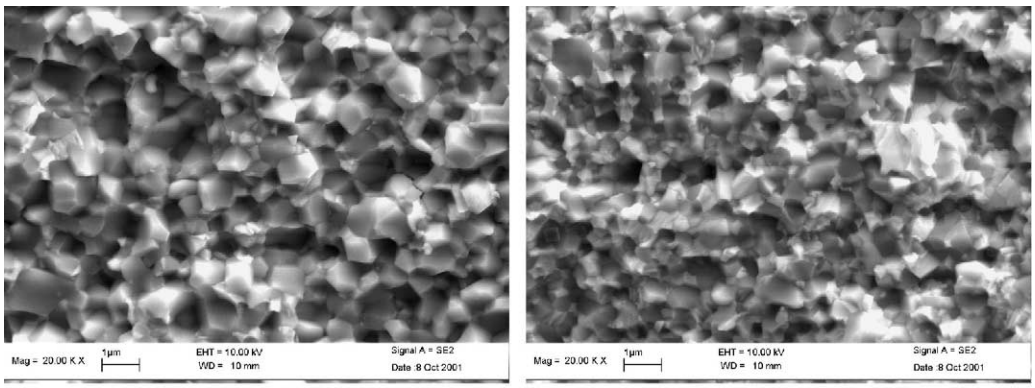

Fig. 8. Fracture surface of 30 and 40 wt.% $Al_2O_3/LaPO_4$ composites.

where G, k, r and f are mean grain size of matrix, constant, mean grain size of second phase and volume fraction of second phase, respectively. Eq. (3) shows that the grain size of matrix depends on particle size and volume fraction of second phase. Eq. (3) clearly suggests that mean grain size (G) decrease with increasing volume fraction (f) of $LaPO_4$. From the microstructure of composites, it was also obvious that the addition of $LaPO_4$ prohibited the abnormal growth of alumina grains.

For the monolithic Al_2O_3 ceramic, fracture mode of some intergranular Al_2O_3 phase was obviously observed (Fig. 7a). Al_2O_3 grain underwent mixed intergranular/transgranular cleavage. At the same time, SEM observations showed that the fracture mode of Al_2O_3 grain in all composites was mainly transgranular. That confirmed the weak bonding of Al_2O_3 and $LaPO_4$. According to the EDAX analysis, $LaPO_4$ phase accumulated at the boundaries of Al_2O_3 grains and formed a weak interface with Al_2O_3 grains because no reaction occurred between two phases. Maybe it is the reason of the improvement of machinability, due to the easily flaking of grain and the extending of fracture route. According to the microstructure evolution, compared with the monolithic Al_2O_3, the composite system possessed narrow and homogeneous grain size distribution, and this tendency became more obvious with increasing $LaPO_4$ content.

3.5. Machinability

Fig. 8 showed the main fracture mode of 30 wt % and 40 wt % $LaPO_4/Al_2O_3$ composite belonging to transgranular fracture. Cracks preferred propagating along interfaces or deflecting into $LaPO_4$. There were many lateral cracks propagating along interfaces, but no crack was propagating perpendicularly through Al_2O_3. This may be the main reason that the addition of $LaPO_4$ improves the machinability of Al_2O_3-based ceramics.

The machinability of $Al_2O_3/LaPO_4$ composites using cemented carbide drills was investigated. Generally, diamond tools are used for the machining of advanced ceramics. Fig. 9 showed a hole made by cemented carbide drills on the 30 wt.% $Al_2O_3/LaPO_4$ specimen. It can be seen that the $Al_2O_3/LaPO_4$ composite was successfully machined. However, due to the high hardness, the pure Al_2O_3 cannot be machined using such drills. As stated above, the layered structure $LaPO_4$ and the weak interface at the $Al_2O_3/LaPO_4$ grain boundaries are the main reason for the improvement of the machinability. Both of them enhance the crack deflection and avoid the catastrophic failure of the material during drilling. Other important factors including the wear of the tool, the cutting force vs drilling rate, the surface roughness of the work piece, the diffusion mechanism between the tool and the work piece, will be studied systematically in the future.

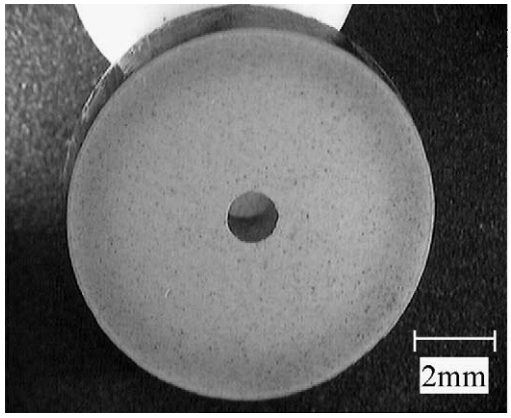

Fig. 9. Hole drilled in 30 wt.%$LaPO_4/Al_2O_3$ composite using cemented carbide drill.

4. Conclusions

Microstructure and mechanical properties development of $Al_2O_3/LaPO_4$ composites have been presented as a function of the $LaPO_4$ content. X-ray diffraction analysis showed that only Al_2O_3 and $LaPO_4$ phases were observed in the $Al_2O_3/LaPO_4$ composites for this

sintering temperature with different $LaPO_4$ concentrations. Layered crystal structure of $LaPO_4$ ceramic was observed. $LaPO_4$ segregation at the Al_2O_3 grain boundaries and layered soft $LaPO_4$ phase can be responsible for the reduction of mechanical properties and improvement of composites machinability. Mechanical properties, sinterability are reduced with increasing $LaPO_4$ content, and microstructure of $Al_2O_3/LaPO_4$ composites became finer and homogenous dependent on the $LaPO_4$ concentration. 30 wt.%$Al_2O_3/LaPO_4$ composite can be easily machined using cemented carbide drill instead of conventional diamond tools.

References

[1] J.B. Davis, D.B. Marshall, P.E.D. Morgan, Oxide composites of Al_2O_3 and $LaPO_4$, J. Eur. Ceram. Soc. 19 (13–14) (1999) 2421–2426.

[2] J.R. Mawdsley, D. Kovar, J.W. Halloran, Fracture behavior of alumina/monazite multilayer laminates, J. Am. Ceram. Soc. 83 (4) (2000) 802–808.

[3] J.B. Davis, D.B. Marshall, P.E.D. Morgan, Monazite-containing oxide/oxide composites, J. Eur. Ceram. Soc. 20 (5) (2000) 583–587.

[4] J.B. Davis, D.B. Marshall, R.M. Housley, P.E.D. Morgan, Machinable ceramics containing rare-earth phosphates, J. Am. Ceram. Soc. 81 (8) (1998) 2169–2175.

[5] Ruigang Wang, Wei Pan, J. Mater. Sci. Eng. A (submitted for publication).

[6] H. Klug, L. Alexander, X-ray diffraction procedures for polycrystalline and amorphous materials, John Wiley and Sons, New York, 1974.

[7] M. Sternitzke, Structural ceramic nanocomposites, J. Eur. Ceram. Soc. 17 (9) (1997) 1061–1082.

[8] D.G. Grossman, Machinable glass-ceramics based on tetrasilicic mica, J. Am. Ceram. Soc. 55 (9) (1972) 446–449.

[9] M.W. Barsoum, et al., Synthesis and characterization of a remarkable ceramic: Ti_3SiC_2, J. Am. Ceram. Soc. 79 (7) (1996) 1953–1956.